Mat. Res. Soc. Symp. Proc. Vol. 692 © 2002 Materials Research Society H10.2

# Space Radiation Effects in Advanced Solar Cell Materials and Devices

R. J. Walters and G. P. Summers
US Naval Research Laboratory, Washington, DC 20375
S. R. Messenger
SFA, Inc., Largo, MD 20000

## ABSTRACT

An investigation of the physical mechanisms governing the response of III-V based solar cells to particle irradiation is presented. The effect of particle irradiation on single and multijunction solar cells is studied through current vs. voltage, spectral response, and deep level transient spectroscopy measurements. The basic radiation response mechanisms are identified, and their effects on the solar cell electrical performance are described. In particular, a detailed analysis of multijunction $In_xGa_{1-x}P/In_yGa_{1-y}As/Ge$ devices is presented. The MJ cell response is found to be more strongly affected by the internal cell structure than by the In content.

## INTRODUCTION

This invited talk will give a brief tutorial on the effects of the space radiation environment on the electrical properties of advanced photovoltaic materials and devices. Solar cells are the basis of nearly all spacecraft power systems. The space market for commercial communications as well as military and scientific applications is driving rapid development of new solar cell technologies to provide increased power. In particular, the approach of multijunction (MJ) solar cells, where bandgap engineering is employed in layering several semiconductor junctions in a monolithic stack, has rapidly matured, attaining record, one-sun, air-mass-zero efficiencies close to 30% [1]. However, for these advanced technologies to operate efficiently in space, they must by resistant to the harsh space radiation environment. This paper will begin with a discussion of the basic mechanisms of radiation damage in solar cell materials. The talk will then describe the physics of multijunction solar cells and show how these advanced devices respond to radiation exposure. In keeping with the general symposium theme, the presentation will focus on the InGaAs and related material systems.

## BASIC RADIATION DAMAGE MECHANISMS

As an energetic particle passes through the atomic lattice of a material, it transfers energy to the lattice through ionizing events in which electrons in the lattice are temporarily excited to higher energy levels and nonionizing events in which collisions between the incident particle and target atoms results in displacement of atoms in the lattice. In terms of solar cell radiation-induced degradation, ionization has little effect. It is the permanent displacement damage produced by nonionizing events that degrades the device electrical performance. A calculation of the amount of energy lost to nonionizing events (i.e. the nonionizing energy loss (NIEL)) by a proton and an electron incident upon GaAs as a function of the incident particle energy is shown in Fig. 1 [2]. The calculated NIEL values show protons to be much more damaging with the amount of damage increasing as the energy decreases until the threshold for

atomic displacement is reached. For electrons, on the other hand, the amount of displacement damage decreases as the energy decreases.

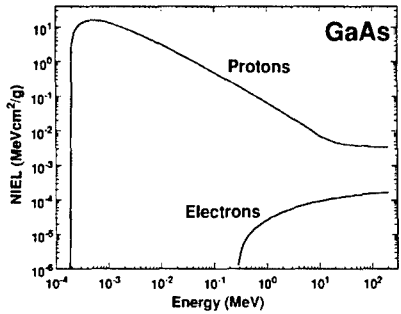


**Figure 1.** Calculated nonionizing energy loss (NIEL) for electrons and protons incident upon GaAs

Considering a solar cell in a space radiation environment, the primary radiation effect is the creation of point defects or defect complexes that form energy levels within the semiconductor bandgap. An example of a radiation-induced defect spectrum as measured in an InP solar cell after proton irradiation using deep level transient spectroscopy (DLTS) is shown in Fig 2 [3]. Each peak in the DLTS spectrum corresponds to a specific defect energy level acting as a trapping center for free charge carriers. A positive peak indicates a majority carrier trap and a negative peak indicates a minority carrier trap.

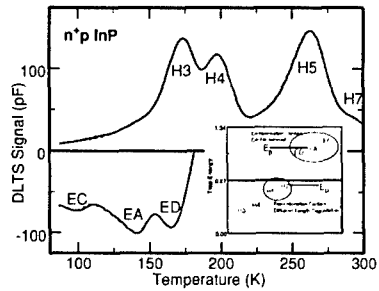


**Figure 2.** Deep level transient spectroscopy (DLTS) measurements made on an InP solar cell after irradiation. The positive peaks indicate a majority carrier trap, and the negative peaks indicate capture of a minority charge carrier. The inset indicates the location of the defect levels within the InP bandgap.

The effects of the radiation-induced defects on the solar cell electrical characteristics depend on the location of the defect energy level within the bandgap. Those defect levels lying nearer to mid-gap, like the defect levels labeled H4 and H5 in the spectrum of Fig. 2, tend to act as free charge carrier traps and recombination centers. The presence of such defect levels reduces the minority carrier lifetime ($\tau$) and diffusion length (L). The decrease in L with the introduction of defects is given by [4]:

$$\frac{1}{L^2(D_d)} = \frac{1}{L_0^2} + \sum \frac{\sigma_i \nu I_{ti}}{D} D_d = \frac{1}{L_0^2} + \kappa_L D_d \qquad \text{Equ (1)}$$

where $L_o$ is the preirradiation value of L, $\sigma_i$ is the minority carrier capture cross section of the $i^{th}$ recombination center, $I_{ti}$ is the introduction rate of the $I^{th}$ recombination center, $\nu$ is the thermal velocity of the minority carrier, D is the diffusion coefficient, and Dd is the displacment damage dose, which is given by the product of the particle fluence and the NIEL [5]. As shown in Eq. (1), the specific parameters for each defect are typically lumped into a single damage coefficient, $K_L$. An example of measured diffusion length data and a fit of the data to Eq. (1) is shown in Fig. 3.

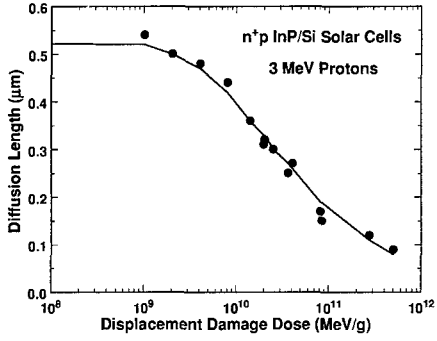


**Figure 3.** Degradation of the minority carrier diffusion length, L, in an InP solar cell due to proton irradiation. The line represents a fit of the data to Equ 1.

Those defects lying closer to one of the bands tend to act as majority charge carrier traps. The capture of a majority carrier can cause compensation of the material thus reducing the carrier concentration. This is referred to as carrier removal and such trapping centers are referred to as compensation centers. Carrier removal effects emerge when the radiation-induced defect concentration is on the order of the dopant concentration. Since solar cells typically have dopant levels $>10^{16}$ $cm^{-3}$, carrier removal effects are usually not seen until relatively higher irradiation levels. In the case of InP, the minority carrier traps labeled EA, EC, and ED (Fig. 4) have been shown to be compensation centers. A demonstration of the evolution of the carrier concentration under irradiation is shown in Fig. 4, where electrochemical capacitance (ECV) profiling has been used to measure the carrier density in an $n^+p$ InP solar cell after increasing levels of irradiation [6]. The irradiation causes the carrier concentration in the p-type material to be reduced until the material is actually type converted and driven n-type.

## BASIC RADIATION DAMAGE MECHANISMS

In this section, the radiation damage mechanisms discussed in the preceding section will be related to the degradation of the electrical output of a solar cell. The primary method for characterizing the output of a solar cell is by measuring the current vs. voltage (IV) curve under simulated solar light. An example of an IV curve measured on a single-junction InP solar cell is shown in Fig. 5. The standard IV parameters extracted from these data are the short circuit current, Isc; the open circuit voltage, Voc; and the maximum power, Pmp. The sunlight to

electricity conversion efficiency (Eff) is determined by dividing Pmp by the incident solar power. In this paper, all measurements were made under extraterrestrial simulated solar light, i.e. air mass zero (AM0), at one sun intensity, 136.7 mW/cm$^2$. The final IV parameter to introduce is the fill factor (FF), which is given by the ratio of Pmp to the product of Isc and Voc and gives a measure of how square the IV curve is. The closer the FF is to unity, the higher the quality of the solar cell junction.

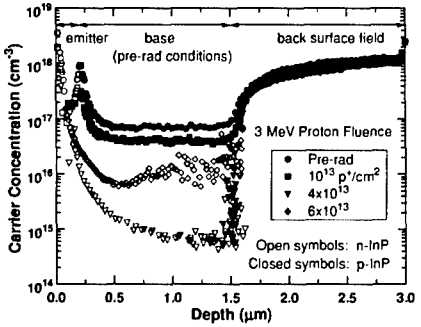


**Figure 4.** Electrochemical capacitance (ECV) profile of an n+p InP solar cell after proton irradiation. The radiation-induced defects act as compensation centers the deplete and then typ-convert the p-type base region.

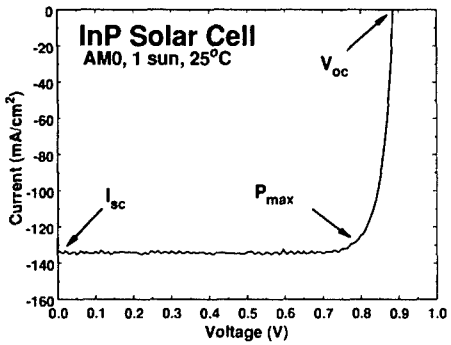


**Figure 5.** Current vs. voltage (IV) curve measured on an InP solar cell indicating the standard IV parameters used to characterize the solar cell electrical output.

When a solar cell is exposed to particle irradiation, the IV parameters degrade. As an example, the decrease in the PV parameters of the InP solar cell of Fig. 5 due to proton irradiation is shown in Fig. 6. For proton fluences up to about 1x10$^{13}$ cm$^{-2}$, each of the IV parameters shows steady degradation. This degradation is due almost entirely to a reduction in the minority carrier diffusion length. As the diffusion length degrades, less of the photogenerated charge carriers are able to transit the material to be collected, so Isc degrades. At the same time, an increase in the concentration of recombination/generation centers in the

depletion region causes an increase in the junction dark current, which degrades Voc. The voltage and current degradation leads to degradation of Pmp and FF.

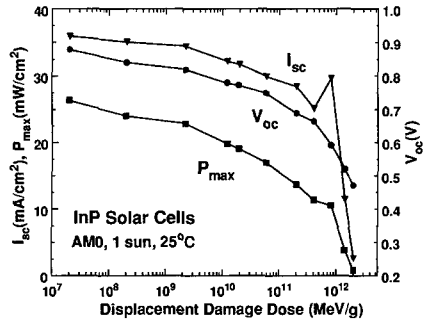


**Figure 6.** Degradation of the IV parameters of an InP solar cell under irradiation.

After irradiation to fluences above $1x10^{13}$ cm$^{-2}$, significantly different behavior is observed. While Voc continues to degrade in a fashion similar to that observed at lower fluences, Isc shows a large increase followed by a decrease to essentially zero. As a result, Pmp experiences a small plateau region followed by a sharp plummet to zero. These effects are caused by carrier removal in the base region. As shown in Fig. 4, at higher fluence levels, the irradiation causes a marked decrease in the base carrier concentration resulting in an increased depletion region width until the entire base region is eventually depleted. In this condition, the carrier collection is entirely by drift along the depletion region electric field, which is much more efficient than collection by diffusion through the bulk material, especially under the condition the reduced carrier lifetime. Therefore, Isc shows an increase. However, the increased size of the depletion region also results in increased recombination/generation dark current, which degrades Voc. When the base material is eventually type converted, the junction is essentially destroyed, and the solar cell stops working. In addition to explaining the solar cell behavior after irradiation to high fluence levels, these results also highlight the influence that the solar cell structure can have on the device radiation response. This will be important in the discussion of multijunction solar cell response below.

## BASIC MULTIJUNCTION SOLAR CELL STRUCTURE

A multijunction (MJ) solar cell is a structure, which consists of a monolithic stack of several semiconductor materials with different bandgaps. The layers are interconnected via tunnel diodes. In this configuration, the voltages of each individual junction add while the current is limited by the junction with the smallest photocurrent. The goal in designing a MJ solar cell is to choose the bandgap combination for maximum electrical conversion of the incident sunlight. A calculation of theoretical efficiencies for a two-junction device as a function of the top and bottom material band gap is shown in Fig. 7. From these calculations it is seen that even with only a two-junction device, efficiencies above 32% are theoretically achievable. However, since these are monolithic devices, the choice of material systems is constrained to ones that allow for high quality growth of one layer upon the other.

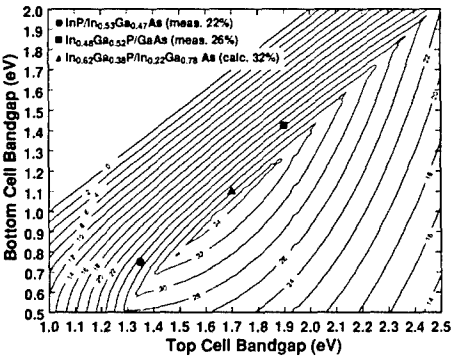


**Figure 7.** Calculated 1 sun, AM0 efficiency of a dual-junction solar cell as a function of top and bottom cell bandgap.

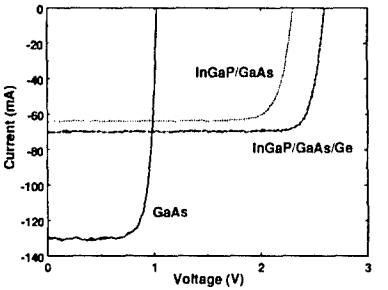


**Figure 8.** Example IV curves a single-junction GaAs/Ge and a dual and triple junction $InGaP_2$/GaAs/Ge solar cells.

By far the greatest success has been achieved with the dual and triple junction $InGaP_2$/GaAs/Ge system. Representative IV curves from a one-junction GaAs/Ge, two-junction $InGaP_2$/GaAs/Ge, and three-junction $InGaP_2$/GaAs/Ge cell are shown in Fig 8. Comparing these curves shows how the addition of the $InGaP_2$ top junction limits the current but boosts Voc by almost 1.3 V resulting in a net increase in power output. Adding a junction in the Ge bottom layer further boosts the voltage by nearly 0.3 V. Since Ge has a relatively low bandgap, the Ge sub-cell typically produces sufficient photocurrent to not limit the overall device current. The current state-of-the-art for the three-junction device has efficiencies approaching 27% (1-sun, AM0) [7].

Efforts to develop higher powered devices include the development of an appropriate 1-eV bandgap material for a forth junction as described in [8]. Other efforts are focused on applying the concept of bandgap engineering to achieve a bandgap combination that is better tuned to the AM0 spectrum (see Fig. 8). Leveraging on the success of the $InGaP_2$/GaAs/Ge technology, the $In_xGa_{1-x}P/In_yGa_{1-y}As$/Ge system is being developed at several laboratories [1,9]. These material system is showing very good results as ongoing improvements in lattice mismatched and strained layer growth techniques are significantly relaxing the lattice matching requirement [10]. Spectral response data measured in $In_xGa_{1-x}P/In_yGa_{1-y}As$/Ge MJ devices at two stoichiometries are shown in Fig. 9. Spectral response is a measurement of the device

response to monochromatic light. Increasing the In content within each subcell, i.e. increasing x and y, decreases the bandgap thus extending the absorption range. This results in increased photo-absorption and, hence, photocurrent, but it also results in reduced voltages. It is balancing these competing effects that yields the stoichiometry that is optimized for a given input spectrum. In addition, the effect of an increased In concentration on the cell radiation response must be considered. This aspect will be investigated in the remainder of the paper.

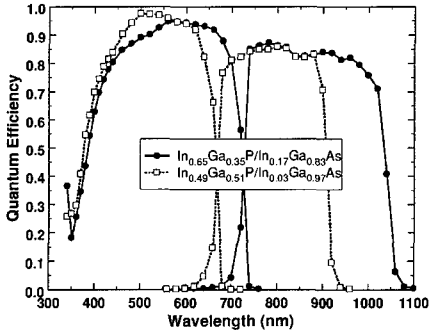


**Figure 9.** Example spectral response curves a dual-junction $In_xGa_{1-x}P/In_yGa_{1-y}As$ solar cells at two stoichiometries.

## MULTIJUNCTION SOLAR CELL RADIATION RESPONSE

An example of the radiation response of MJ $InGaP_2/GaAs/Ge$ devices in both a two and a three-junction configuration is shown in Fig 10 along with data from a single junction GaAs/Ge device for comparison [11,12]. Comparing the data on an absolute scale (Fig 10a) shows that clear advantage of the MJ devices, as the MJ cells produce significantly higher power both before and after irradiation. Comparing Fig 10 with Fig. 6, the MJ cell response is seen to be controlled primarily by diffusion length degradation. Comparing the data on a normalized scale (Fig 10b) shows the degradation characteristics of the three technologies to be similar with the MJ devices showing higher radiation resistance.

The mechanisms for the MJ cell radiation response stems from the monolithic nature of the MJ device. Since the current of a MJ device is limited by the smallest photocurrent of the three sub-junctions, the most radiation sensitive sub-junction generally controls the radiation response. To show this explicitly, the spectral response of an $InGaP_2/GaAs/Ge$ three-junction cell after proton irradiation is considered (Fig 11). The integral of each of these curves with the incident spectrum yields the photocurrent. Given the wide absorption range of the Ge sub-cell, it produces significantly more photocurrent than the top two junctions, even after irradiation, so it does not limit the current. The photocurrents of the top two sub-cells, on the other hand, are quite closely matched in the as-grown device. The as-grown condition is referred to as beginning-of-life (BOL). Indeed, current matching is the condition for maximum power output, and this device was specifically designed to achieve current matching at BOL. However, under irradiation, the GaAs sub-cell degrades much faster than the $InGaP_2$ sub-cell so that it limits the current. This explains the similarity in the normalized radiation degradation curves (Fig 10b), since in each of the three configurations, it is the GaAs junction that controls the radiation response.

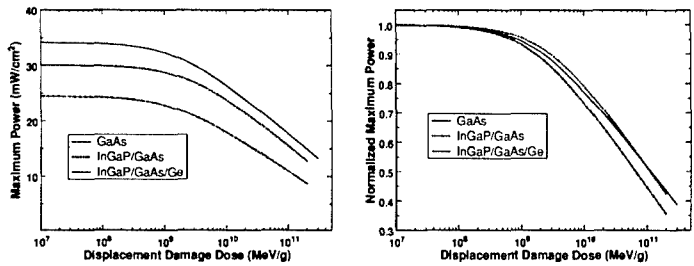


(a) (b)

**Figure 10.** Radiation-induced degradation of single-junction GaAs/Ge and dual and triple-junction GaInP2/GaAs/Ge solar cells considered on an absolute (a) and a normalized scale (b).

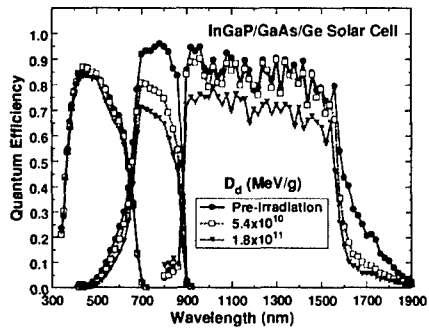


**Figure 11.** Radiation-induced degradation of spectral response of a triple-junction $GaInP_2$/GaAs/Ge solar cell.

The improved radiation resistance of the MJ cells over the single-junction GaAs cells can be explained through current matching. While the cell of Fig. 11 was designed to be current matched at BOL, the cell can also be designed to be current-matched after irradiation. The after irradiation condition is referred to as end-of-life (EOL). Since the GaAs cell degrades more rapidly, a current matched cell at EOL will be top cell limited at BOL. This will sacrifice some of the BOL power but result in optimum EOL performance. Some ways of attaining a top-cell limited device include thinning the top cell, decreasing absorption in the interconnecting tunnel junction, and extending the GaAs sub-cell absorption range. When top-cell limited at BOL, the degradation of a MJ cell will be controlled by the more radiation resistant $InGaP_2$ top-cell until a specific irradiation level is reached where the photocurrent of the GaAs sub-cell is degraded to the level of the top-cell leaving the device current matched. The challenge, then, is to engineer the cell structure so that the radiation level corresponding to current matching coincides with the predicted radiation level of a specific space mission.

## RADIATION RESPONSE OF $In_xGa_{1-x}P/In_yGa_{1-y}As$/Ge MJ SOLAR CELLS

Since the GaAs sub-cell has been shown to be the most radiation sensitive within the $InGaP_2$/GaAs/Ge stack, significant research is being dedicated to understanding the radiation response of single-junction $In_yGa_{1-y}As$ devices for application in the $In_xGa_{1-x}P/In_yGa_{1-y}As$/Ge system. [9,13,14]. The radiation response of several configurations of this cell type is shown in Figs. 12a-c. For Dd levels up to ~ $10^{10}$ MeV/g, the Pmp degradation for all of the $In_yGa_{1-y}As$ cells is nearly equivalent to that of a conventional GaAs cell (i.e. with y=0). This is quite a high exposure level, being roughly equivalent to a one-year mission in the heart of the Earth's proton belts. This indicates the radiation resistance of the $In_yGa_{1-y}As$ cells to be relatively insensitive to changes in the value of y.

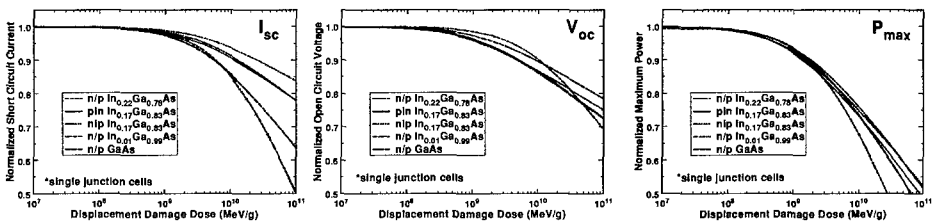


**Figure 12.** Radiation-response of several single-junction $In_yGa_{1-y}As$ solar cells.

Some variation in cell response amongst the different technologies is observed at higher Dd levels. In particular, the 22% In cells showed a rapid decrease in voltage (Fig 12b) and current (Fig 12c) for Dd > $5x10^9$ MeV/g. Measurements showed the Voc degradation to be due to a more rapid radiation-induced increase in dark current in the 22% In cells. This may be a direct result of the higher In content in those cells and, hence, lower band-gap and larger lattice mismatch. However, the $I_{sc}$ response suggests that differences in cell structure also significantly impact the radiation response. The 17% In cells, which were of a p-i-n and n-i-p structure, displayed a much better blue response before irradiation, which was nearly insensitive to the irradiation, and after irradiation, those cells showed a better spectral response at nearly all wavelengths (Fig 13). This can be explained by the enhanced collection efficiency afforded by the intrinsic layer of these cells and to a better front and rear interface passivation scheme. From these results, it can be concluded that, within the range of In concentrations studied, the response of these cells are more strongly controlled by the cell structure than the In concentration.

The radiation response of several dual junction $In_xGa_{1-x}P/In_yGa_{1-y}As$ devices are shown in Fig 12. The device with y = 0.49 and x = 0.0 is an EOL optimized cell developed under the ManTech program [11]. Except for the $In_{0.65}Ga_{0.35}P/In_{0.17}Ga_{0.83}As$ cell in the n/p structure, the cells show generally similar radiation characteristics, independent of the In concentration. This is especially significant in the case of y = 0.35, x = 17 device, considering the large difference in In concentration and the top cell configuration. The n/p $In_{0.65}Ga_{0.35}P/In_{0.17}Ga_{0.83}As$ cell was optimized for terrestrial use under AM1.5 illumination, so the middle cell base thickness and dopant level were larger than optimal for good radiation resistance. These results are similar to those of the single junction $Ga_yIn_{1-y}As$ cells, and again suggest that the cell structure may have considerably more affect on the radiation response than the In concentration.

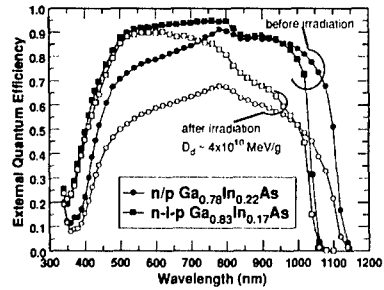


**Figure 13.** Radiation-response of the spectral response of two single-junction $In_yGa_{1-y}As$ solar cells.

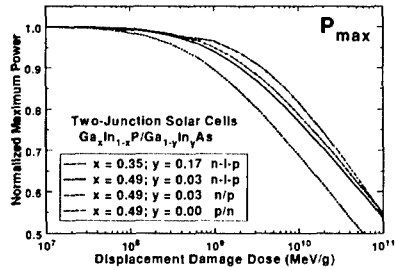


**Figure 14.** Comparison of the radiation-response of several dual junction $In_xGa_{1-x}P/In_yGa_{1-y}As$ solar cells.

The advantages of the EOL optimized $InGaP_2/GaAs$ can be seen through a study of the Isc response of the cells (Fig. 13). At low Dd levels, the Isc of the EOL optimized cell is limited by the top cell, and as such, degrades little since the top cell is quite resistant to irradiation. As the bottom cell degrades at higher Dd levels, the dual-junction device transitions to being bottom cell limited. At this point, the dual-junction Isc degradation curve turns over and rapidly degrades down to the level of the other cells.

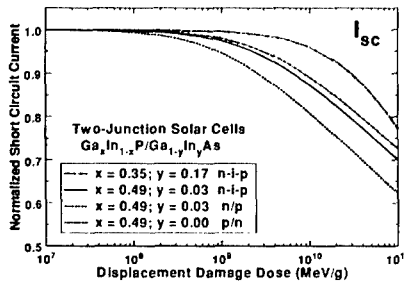


**Figure 15.** Comparison of the radiation-response of Isc in the $In_xGa_{1-x}P/In_yGa_{1-y}As$ solar cells of Fig 12.

These results clearly demonstrate that, like the $InGaP_2/GaAs$ technology, the $Ga_yIn_{1-y}As$ sub-cell cell primarily controls the radiation response of the MJ $Ga_xIn_{1-x}P/Ga_yIn_{1-y}As$ devices. In Fig. 14, the normalized degradation of the Isc of the $Ga_xIn_{1-x}P$ top and $Ga_yIn_{1-y}As$ bottom cells are shown independently. These data were calculated by integrating the spectral response of each subcell over the energy dependence of the AM0 spectrum. The degradation of all the $Ga_xIn_{1-x}P$ cells can be seen to be small up to high damage levels, independent of the stoichiometry. The $Ga_{1-x}In_xAs$ cells, on the other hand, degrade significantly. Also, a significant difference is observed in the degradation of the different $Ga_{1-x}In_xAs$ bottom cells. Since two cell structures, each with y = 0.03, show significantly different behavior, this difference cannot be attributed only to the cell stoichiometry. Again, the cell response appears to be more strongly controlled by the cell structure. The n-i-p $Ga_{0.97}In_{0.03}As$ sub-cell benefits from the increased carrier collection efficiency afforded by the extended electric field of the intrinsic region. Also, in contrast to the n-i-p $Ga_{0.97}In_{0.03}As$, which was designed for AM0 operation, the n/p $Ga_{0.97}In_{0.03}As$ cell was designed from AM1.5 operation, so the base dopant level was relatively high in that cell ($\sim 2x10^{17}$ $cm^{-3}$), which results in a lower radiation resistance.

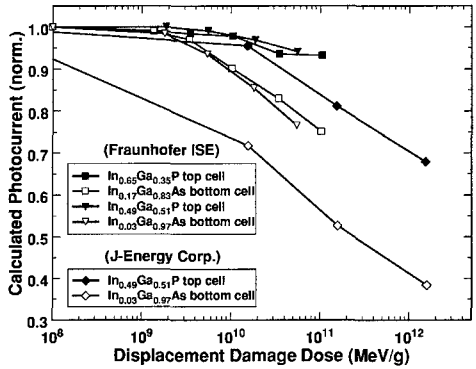


**Figure 16.** Comparison of the radiation-response of photocurrent of the top and bottom cells of the the $In_xGa_{1-x}P/In_yGa_{1-y}As$ solar cells of Figs 12 and 13.

## CONCLUSIONS

In this paper, an comprehensive analysis of the radiation response characteristics of III-V multijunction solar cells has been presented. The basic mechanisms governing the cell radiation response have been identified, and their impact on the cell electrical performance has been described. Results on the electrical performance and radiation hardness of tandem solar cells from the new lattice mismatched $Ga_xIn_{1-x}P/Ga_yIn_{1-y}As$ material combination has been presented. It was shown that despite the lattice mismatch, excellent, multijunction photovoltaic devices can be produced with these material systems. Contrary to initial speculation, the radiation-response of the $Ga_yIn_{1-y}As$-based devices is quite good and essentially independent of In content. Instead, it is the cell structure that more significantly controls the radiation-response, and it has been shown how the cell structure may be optimized for maximum BOL and EOL performance that is equal to or better than conventional $Ga_{0.49}In_{0.51}P/GaAs$ cells.

## REFERENCES


[1] R.R. King, N.H. Karma, J.H. Ermer, M. Haddad, P. Colter, T. Isshiki, H. Ion, H.L. Cotal, D.E. Joslin, D.D. Krut, R. Sudharsanan, K. Edmondson, B.T. Cavicchi, and D.R. Lillington, "Next-Generation, High-Efficiency III-V Multijunction Solar Cells", *Proceedings of the 28th Photovoltaic Specialists Conference*, Anchorage, AK, September, 2000, p. 998.

[2] S.R. Messenger, E.A. Burke, G.P. Summers, M.A. Xapsos, R.J. Walters, E.M. Jackson, and B.D. Weaver, "Nonionizing Energy Loss (NIEL) for Heavy Ions", *IEEE Transactions on Nuclear Science* 46, 1595 (1999).

[3] R.J. Walters and G.P. Summers, "Deep Level Transient Spectroscopy Study of Proton-Irradiated p-Type InP", *J. Appl. Phys.* 69, 6488 (1990).

[4] H.Y. Tada, J.R. Carter, Jr., B.E. Anspaugh, and R.G. Downing, *Solar Cell Radiation Handbook*, 3rd Edition, JPL Publication 82-69, 1982.

[5] G.P. Summers, E.A. Burke, and M.A. Xapsos, "Displacement Damage Analogs to Ionizing Radiation Effects", *Radiation Measurements*, 24, 1 (1995)

[6] S.R. Messenger, E.M. Jackson, E.A. Burke, R.J. Walters, M.A. Xapsos, and G.P. Summers, "Structural Changes in InP/Si Solar Cells Following Irradiation with protons to Very High Fluences", *J. Appl. Phys.* 86, 1230 (1999).

[7] See product literature from the three major US multijunction cell vendors at www.spectrolab.com, www.emcore.com, and www.tecstar.com.

[8] J.M. Olson, J.F. Geisz, S.R. Kurtz, and A.G. Norman, "1-eV semiconductors for multijunction solar cells" ,this conference.

[9] S.R. Messenger, R.J. Walters, G.P. Summers, A.W. Bett, F. Dimroth, C. Baur, M. Meusel, T. Takamoto, T. Agui, M. Imaizumi, and S. Matsuda, "Radiation Response Analysis of Triple Junction InGaP/InGaAs/Ge Solar Cells", *Proceedings of the 17th European Photovoltaic Science and Engineering Conference*, Munich, Germany, October, 2001.

[10] J.A. Carlin, S.A. Ringel, and E.A. Fitzgerald, "Impact of GaAs Buffer Thickness on Electronic Quality of GaAs Grown on Graded Ge/GeSi/Si Substrates", *Appl. Phys. Lett.* 76, 1884 (2000).

[11] D. C. Marvin, Aerospace Report: TOR-00(1210)1

[12] B. E. Anspaugh, Proc. 22nd IEEE Photovoltaic Specialist Conference, Las Vegas, NV, Oct. 1991, p. 1593

[13] R.J. Walters, S.R. Messenger, G.P. Summers, A.W. Bett, F. Dimroth, R.W. Hoffman, Jr., M.A. Stan, T. Takamoto, E. Ikeda, M. Imaizumi, O. Anzawa, and S. Matuda, "Radiation Response of $Ga_xIn_{1-x}As$ Solar Cells", *Proceedings of the 16th European Photovoltaic Science and Engineering Conference*, Glasgow, United Kingdom, May, 2000.

[14] F. Dimroth, A.W. Bett, R.J. Waletrs, G.P. Summers, S.R. Messenger, T. Takamoto, E. Ikeda, M. Imaizumi, O. Anzawa, and S. Matsuda, "Radiation Response of Dual-Junction $Ga_yIn_{1-y}P/Ga_{1-x}In_xAs$ Solar Cells", *Proceedings of the 28th Photovoltaic Specialists Conference*, Anchorage, AK, September, 2000, p. 1110